



King Saud University
Arabian Journal of Chemistry

www.ksu.edu.sa
www.sciencedirect.com



ORIGINAL ARTICLE

Synthesis and photoluminescent properties of a Schiff-base ligand and its mononuclear Zn(II), Cd(II), Cu(II), Ni(II) and Pd(II) metal complexes

E.S. Aazam ^{a,*}, A.F. EL Hussein ^b, H.M. Al-Amri ^a

^a Department of Chemistry, Girls Section, University of King Abdulaziz, P.O. Box 6171, Jeddah 21442, Saudi Arabia

^b Department of Chemistry, Faculty of Science, Alexandria University, Egypt

Received 19 July 2010; accepted 20 July 2010

Available online 14 August 2010

KEYWORDS

Schiff base;
Mononuclear M(II);
Square planar;
Tetrahedral;
Octahedral;
ESR;
Coumarin;
Photoluminescence

Abstract Mononuclear Zn(II), Cd(II), Cu(II), Ni(II) and Pd(II) metal complexes of Schiff-base ligand(HL₁) derived from 8-acetyl-7-hydroxycoumarin and *P*-phenylenediamine were prepared and characterized by microanalytical, mass, UV–Vis, IR, ¹H NMR, ¹³C NMR, ESR, conductance and fluorescence studies. The measured low molar conductance values in DMSO indicate that the complexes are non-electrolytes. The structures of the solid complexes under study are established by using IR, electronic and ESR spectroscopy suggesting that Zn(II) and Ni(II) complexes are octahedral, Cd(II) complex is tetrahedral, Cu(II) and Pd(II) complexes are square planar. The ESR spectrum of the Cu(II) complex in DMSO at 298 and 150 K was recorded and its salient features are reported, it supports the mononuclear structure. The Schiff base exhibited photoluminescence originating from intraligand (π–π*) transitions. Metal-mediated enhancement is observed on complexation of HL with Zn(II) and Cd(II), whereas metal-mediated fluorescence quenching occurs in Cu(II), Ni(II) and Pd(II).

© 2010 King Saud University. Production and hosting by Elsevier B.V. All rights reserved.

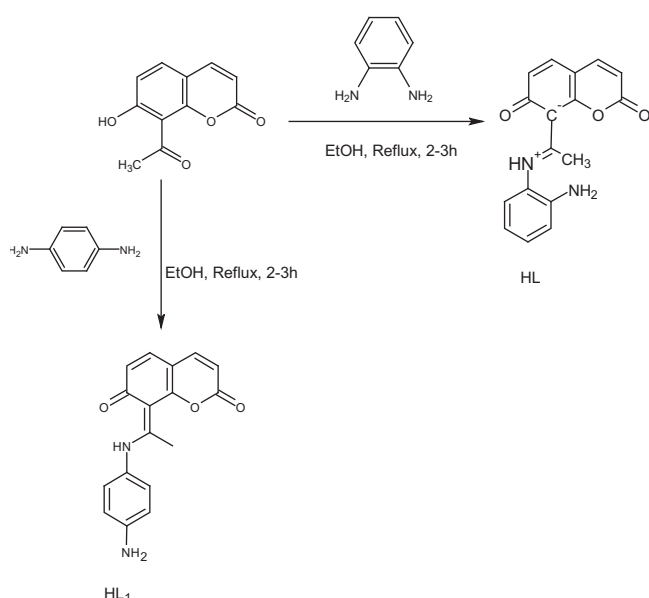
* Corresponding author. Tel.: +966 509695379.
E-mail address: wayfield8@yahoo.com (E.S. Aazam).



1. Introduction

Metal-chelate Schiff-base complexes have continued to play the role of one of the most important stereochemical models in main group and transition metal coordination chemistry due to their preparative accessibility, diversity and structural variability (Garnovskii et al., 1993). Coumarin-derived Schiff bases are well-known compounds and several reports have been written about their applications as dye and fluorescent agents (Kachkovski et al., 2004; Creaven et al., 2009). We have recently reported synthesis, spectroscopic characterization and antimicrobial studies of a series of polydentate ligands and

their copper(II) complexes and discovered that 8-[1-(2-amino-phenylimino)-ethyl]-7-hydroxy-chromen-2-one, (HL) Cu(II) complex [LCu(OAc)] is a promising alternative antimicrobial agent due to its safe application in both human health and ecosystem (EL Hussein et al., in press). However, the complexation and photophysical properties of the ligand 8-[1-(4-amino-phenylimino)-ethyl]-7-hydroxy-chromen-2-one, (HL₁) still need to be explored. Our choice of coumarin as the fluorophore is based on the fact that it possesses desirable photophysical properties such as a large Stokes shift and visible excitation and emission wavelengths. This research is also concerned with the first exploration of the coordination chemistry of the free ligand complexes synthesized and characterized via exposure to analytical techniques in an attempt to elucidate the coordination mode of the organic ligand and the structure of its metal complexes. This was investigated by means of mass spectrometry, and spectroscopic methods such as: Fluorescence, IR, UV/vis, ¹³C NMR and ¹H NMR. The promising fluorescent results obtained reflect the rich and versatile application chemistry of the system.



Scheme 1 Synthesis of HL and HL₁.

2. Experimental

Bis(benzonitrile)-dichloro-palladium(II) was obtained from Fluka; 8-acetyl-7-hydroxy-coumarin was purchased from Sigma-Aldrich; copper(II) acetate monohydrate, zinc(II) acetate dehydrate, cadmium(II) acetate dehydrate, nickel(II) chloride hexahydrate, nickel(II) acetate tetra hydrate, palladium(II) acetate, *P*-phenylenediamine were procured from BDH. Methanol, ethanol, dimethylsulphoxide and diethyl ether were of pure grade and used as submitted from BDH.

2.1. Physical measurements

Infrared spectra of solids were recorded in the region 4000–650 cm^{−1} on a Perkin Elmer Spectrum 100 FT-IR spectrometer. Electronic absorption spectra were recorded in the 200–900 nm region in a JASCO V-530 UV/vis spectrophotometer. Fluorescence spectra were recorded on a Perkin Elmer LS-55 spectrometer at room temperature (298 K) in DMSO solution with a 1 cm path length quartz cell. The molar conductance measurements of 10^{−3} M metal(II) complexes in DMSO were carried out using Fisher Conductometer model AP75 with Cell constant equal to 1 cm^{−1}. Elemental analysis of carbon, hydrogen and nitrogen was determined in the Micro Analytical Unit using Perkin Elmer 2400. The metal ion content was determined using ICP (Inductively Coupled Plasma) – Optical Emission Spectrometer; model Optima 4100 DV, Perkin Elmer. Melting points were carried out on a melting point apparatus, Gallenkamp, England. Perkin Elmer TGA7. Thermogravimetric analyzer was used to record simultaneously TG and DTG curves. Solution NMR spectra were recorded using an AM-500 Bruker spectrometer with TMS or DMSO-d₆ was used as an internal standard and the chemical shifts are given in parts per million (ppm). EPR spectra were recorded on Bruker ESP-300 and JEOL JESRE – IX with variable temperature unit.

2.2. Synthesis of 8-(1-(4-aminophenylamino)ethylidene)-2H-chromene-2,7(8H)-dione, HL₁

A clear solution of *P*-phenylenediamine (0.13 g, 1.22 mmol) in 10 ml of ethanol was added to a warm solution of 8-acetyl-7-hydroxycoumarin (0.50 g, 2.44 mmol) in the same solvent (30 ml) (Scheme 1). The resulting mixture was refluxed for 2–3 h. The yellow product was precipitated, filtered off and washed with ethanol followed by diethyl ether, dried in a vacuum desiccator and crystallized from chloroform/ethanol

Table 1 Elemental analysis and physical data of HL₁ ligand and its metal complexes.

Compound	Formula	Color	Elemental Analysis Cal (Found)				Molar conductance (Ω ^{−1} cm ² mol ^{−1})
			%C	%H	%N	%M	
HL ₁	C ₁₇ H ₁₄ N ₂ O ₃	Yellow	69.38 (68.89)	4.76 (4.33)	9.52 (9.04)	–	–
[ZnHL ₁ (OAc) ₂ (H ₂ O) ₂]	C ₂₁ H ₂₄ N ₂ O ₉ Zn	Pale yellow	49.08 (49.57)	4.67 (3.64)	5.45 (4.92)	12.74 (12.32)	2.63
[CdHL ₁ (OAc) ₂ ·2H ₂ O]	C ₂₁ H ₂₄ N ₂ O ₉ Cd	Green	44.97 (45.39)	4.28 (3.38)	5.00 (4.39)	20.06 (20.17)	4.37
[CuHL ₁ (OAc) ₂]	C ₂₁ H ₂₀ N ₂ O ₇ Cu	Brown	53.00 (53.13)	4.20 (4.00)	5.88 (5.87)	13.35 (12.97)	2.80
[NiHL ₁ Cl ₂ (H ₂ O) ₂]	C ₁₇ H ₁₈ Cl ₂ N ₂ O ₅ Ni	Green	44.38 (44.02)	3.92 (3.21)	6.09 (5.57)	12.77 (12.28)	4.55
[PdHL ₁ Cl ₂]	C ₁₇ H ₁₄ Cl ₂ N ₂ O ₃ Pd	Green	43.28 (44.80)	3.97 (2.37)	5.94 (5.48)	22.57 (22.18)	2.7

The decomposition melting point for all complexes was > 300 °C.

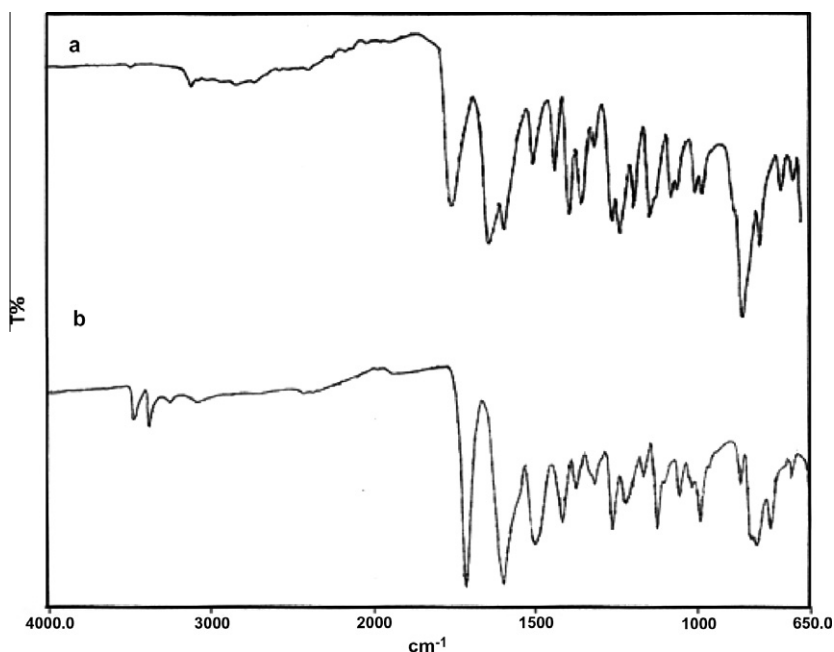


Figure 1 Infrared spectra of (a) 8-acetyl-7-hydroxycoumarin AND (b) HL₁.

Table 2 Infrared data of HL₁ and its metal complexes.

Compound	IR (ν , cm^{-1})					
	$\nu(\text{C}=\text{O})$	$\nu(\text{C}=\text{N})$	$\nu(\text{C}-\text{N})$	$\nu(\text{C}-\text{O})$	$\nu_{\text{asym}}(\text{C}-\text{O}-\text{C})$	$\nu_{\text{asym}}(\text{NH}_2)$, $\nu_{\text{sym}}(\text{NH}_2)$ or $\nu(\text{NH})$
HL ₁	1710	1590	1125	1221	1054	3463, 3364
[ZnHL ₁ (OAc) ₂ (H ₂ O) ₂]	1709	1565	1124	1230	1055	3458, 3368
[CdHL ₁ (OAc) ₂].2H ₂ O	1709	1570	1128	1235	1058	3460, 3359
[CuHL ₁ (OAc) ₂]	1707	1571	1125	1243	1055	3467, 3356
[NiHL ₁ Cl ₂ (H ₂ O) ₂]	1710	1568	1127	1240	1059	3462, 3366
[PdHL ₁ Cl ₂]	1705	1569	1131	1235	1060	3457, 3356

(2:1). Yield (80%), m.p. (217) °C. Purity of the ligand was checked using TLC; (methanol:benzene, 1:4).

2.3. Preparation of metal complexes

A solution of HL₁ (0.10 g, 0.34 mmol) in ethanol was adjusted to about pH 8 with 0.1 M of potassium hydroxide and then (0.07 g, 0.34 mmol) zinc(II) acetate, (0.09 g, 0.34 mmol) cadmium(II) acetate, (0.07 g, 0.34 mmol) copper(II) acetate, (0.08 g, 0.34 mmol) nickel(II) chloride, (0.13 g, 0.34 mmol) bis(benzonitrile)-dichloro-palladium(II) in ethanol (15 ml) were added; the resulting mixture was refluxed for 10 min, followed by filtration and washing of the instantly formed precipitate thoroughly with methanol. The product was then dried in a vacuum desiccator over CaCl₂. The elemental analysis of the organic ligand and its metal complexes is tabulated in Table 1. The solid complexes were stable in air, insoluble in water, slightly soluble in alcohols and in all common organic solvent and freely soluble in warm DMSO. The observed lower molar conductivity value for metal complexes revealed their non-electrolytic nature (Refat et al., 2008) (Table 1).

3. Results and discussion

3.1. Infrared absorption spectra

The infrared spectrum of 8-acetyl-7-hydroxycoumarin showed a weak band in the region 3600–2300 cm^{-1} attributed to intramolecular hydrogen bonding between the 7-hydroxy and 8-acetyl group (Fig. 1). The IR spectrum of the Schiff base showed characteristic bands for C=N, C=O and C–O vibrations (Table 2). The signals appearing at ν 3364 and 3463 cm^{-1} in HL₁ spectrum were assigned to $\nu_{\text{sym}} \text{NH}_2$ and $\nu_{\text{asym}} \text{NH}_2$, respectively. These bands remained unchanged in all metal complexes, thus excluding coordination of the ligand through the amine group (Fig. 2) (Donia et al., 2003). The $\nu(\text{C}=\text{N})$ and $\nu(\text{C}-\text{O})$ for metal complexes exhibited a downward shift (15–45 cm^{-1}) and (9–22 cm^{-1}), respectively, thus supporting the participation of the azomethine group and the formation of M–O bonds via deprotonation (Bagihalli et al., 2008). While $\nu(\text{C}=\text{O})$ and $\nu_{\text{asym}}(\text{C}-\text{O}-\text{C})$ of the complexes remained as in HL₁, thus excluding their participation in chelate formation (Table 2 and Fig. 2). The bands observed at 1514–1545 cm^{-1}

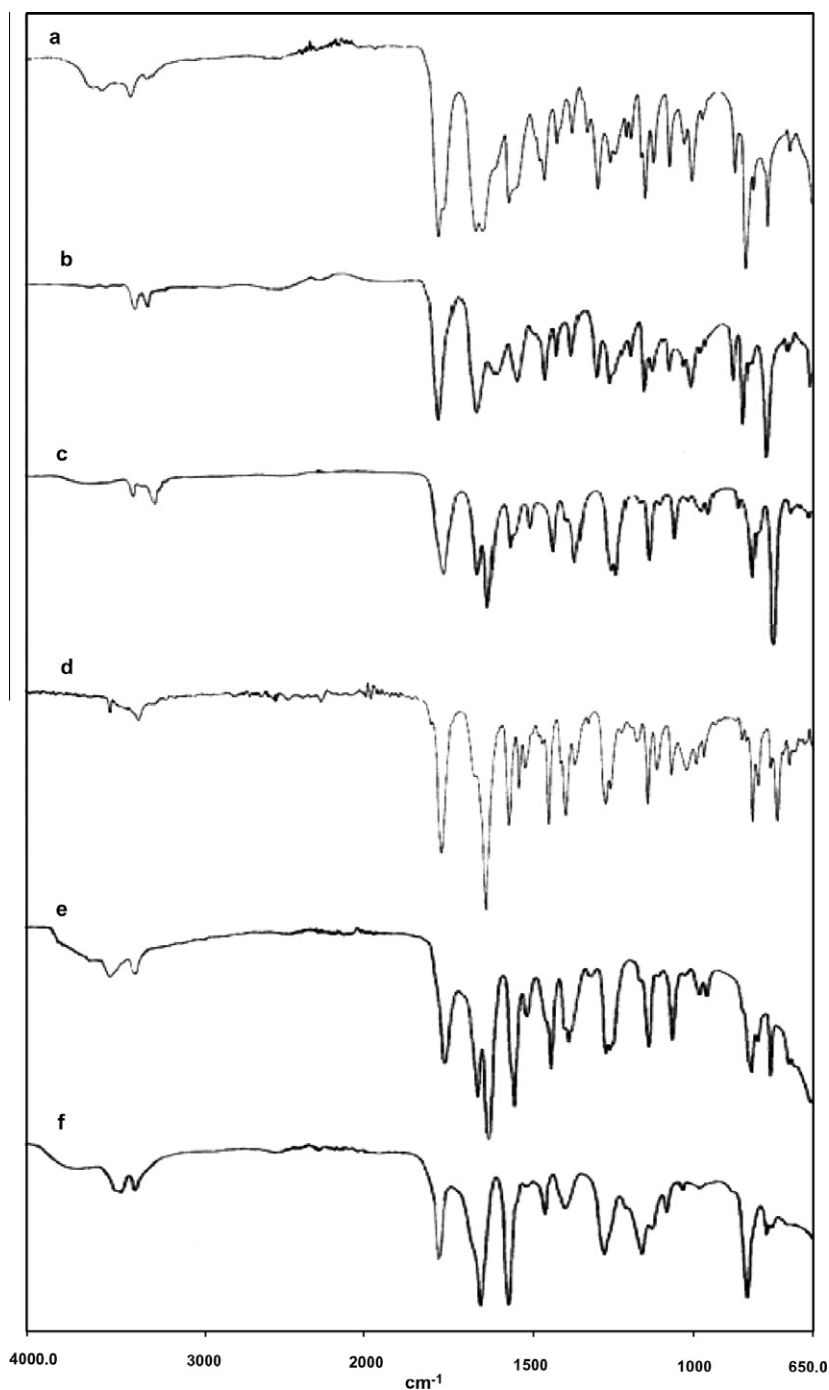


Figure 2 Infrared spectra of (a) HL_1 , (b) $[\text{ZnHL}_1(\text{OAc})_2(\text{H}_2\text{O})_2]$, (c) $[\text{CdHL}_1(\text{OAc})_2] \cdot 2\text{H}_2\text{O}$, (d) $[\text{CuHL}_1(\text{OAc})_2]$, (e) $[\text{NiHL}_1\text{Cl}_2(\text{H}_2\text{O})_2]$ and (f) $[\text{PdHL}_1\text{Cl}_2]$.

and $1402\text{--}1408\text{ cm}^{-1}$ in the spectra of $[\text{ZnHL}_1(\text{OAc})_2(\text{H}_2\text{O})_2]$, $[\text{CdHL}_1(\text{OAc})_2] \cdot 2\text{H}_2\text{O}$ and $[\text{CuHL}_1(\text{OAc})_2]$ were assigned to $\nu_{\text{as}}(\text{COO}^-)$ and $\nu_{\text{s}}(\text{COO}^-)$ of acetate group, respectively. The magnitude of separation between these two vibrations ($\Delta\nu = 112\text{--}137\text{ cm}^{-1}$) suggests the binding of acetate to the metal in a monodentate fashion (Lever and Ogden, 1967). The IR spectra of $\nu(\text{H}_2\text{O})$ of coordinated water appeared at $825\text{--}846\text{ cm}^{-1}$, indicating the binding of water molecules to the metal ions.

3.2. Thermal studies

Thermogravimetric (TG) and differential thermogravimetric (DTG) analyses were carried out for $[\text{ZnHL}_1(\text{OAc})_2(\text{H}_2\text{O})_2]$ and $[\text{CdHL}_1(\text{OAc})_2] \cdot 2\text{H}_2\text{O}$ complexes in the $800\text{ }^\circ\text{C}$ range under N_2 atmosphere. Typical TG and DTG curves are presented in Figs. 3 and 4. Thermal data of the complexes are given in Table 3. The correlation between the different decomposition steps of the complexes with the corresponding weight

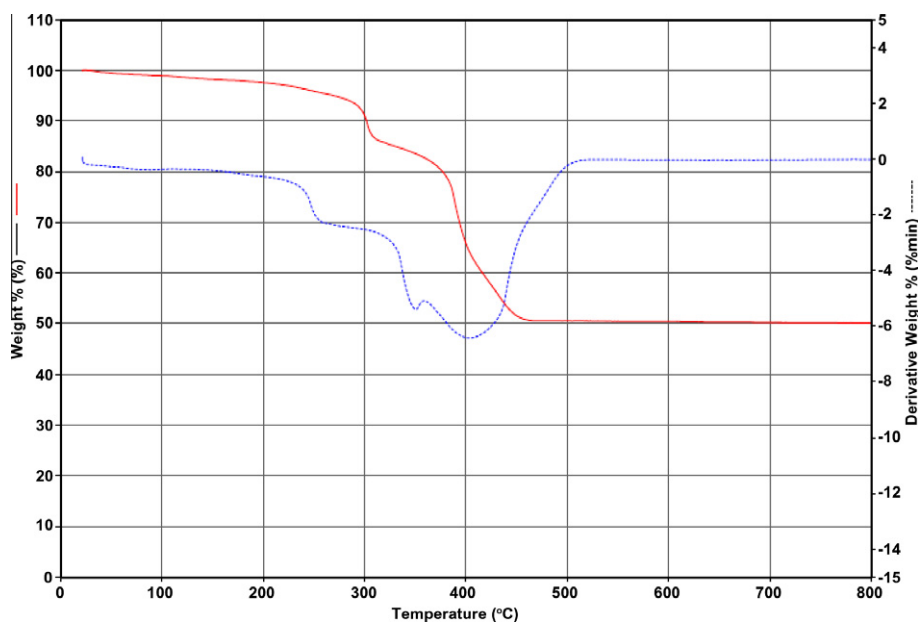


Figure 3 TG and DTG curves of $[\text{ZnHL}_1(\text{OAc})_2]\cdot 2\text{H}_2\text{O}$.

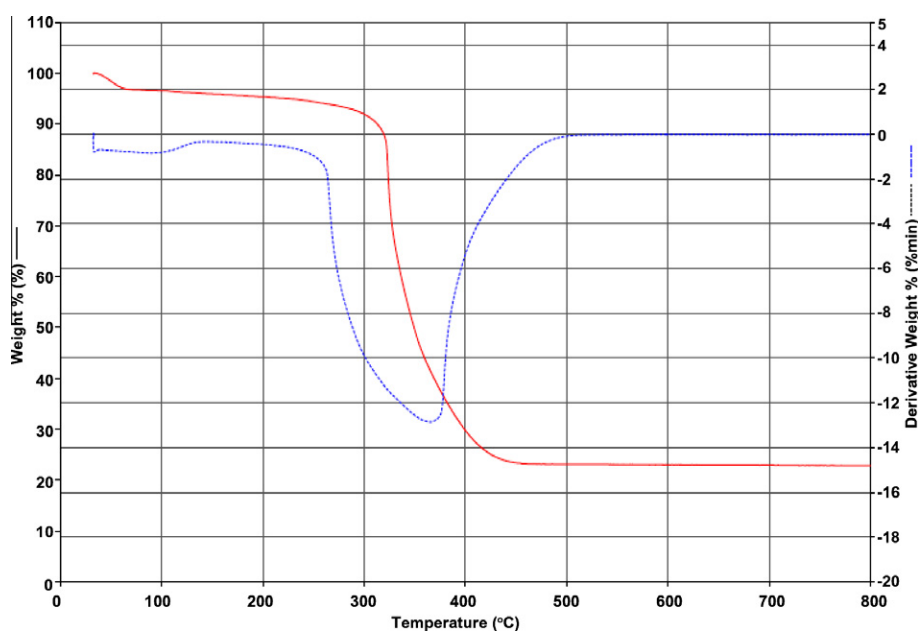


Figure 4 TG and DTG curves of $[\text{CdHL}_1(\text{OAc})_2]\cdot 2\text{H}_2\text{O}$.

Table 3 Thermogravimetric data of metal complexes.

Complex	TG range (°C)	DTG _{max} (°C)	% Estimated (calculated)		Assignment
			Mass loss	Total mass loss	
$[\text{ZnHL}_1(\text{OAc})_2]\cdot 2\text{H}_2\text{O}$	22–306	257	12.49 (12.47)	49.90 (50.26)	Loss of $2\text{H}_2\text{O} + \text{CO}$
	306–385	358	10.20 (10.13)		Loss of $\text{CH}_3\text{OH} + \text{NH}_2 + 2\text{H}_2$
	385–486	404	27.21 (27.66)		Loss of $\text{C}_9\text{H}_4\text{ON}$
			50.12 (49.77)		Metal acetate + 6C (Residue)
$[\text{CdHL}_1(\text{OAc})_2]\cdot 2\text{H}_2\text{O}$	33–90	80	6.10 (6.43)	76.90 (77.09)	Loss of $2\text{H}_2\text{O}$
	263–480	365	70.80 (70.66)		Loss of $\text{C}_{21}\text{H}_{20}\text{N}_2\text{O}_6$
			23.17 (22.95)		CdO (Residue)

losses is discussed in terms of the proposed formula of the complexes.

The TG and DTG curves of $[\text{ZnHL}_1(\text{OAc})_2(\text{H}_2\text{O})_2]$ complex with molecular formula $[\text{C}_{21}\text{H}_{24}\text{N}_2\text{O}_9\text{Zn}]$ are shown in Fig. 3 and Table 3. The TG shows three stages of decomposition within temperature range 22–800 °C. The first step of decomposition in the temperature range 22–306 °C shows that a mass loss 12.49% (calculated mass loss = 12.47%) corresponds to loss of $2\text{H}_2\text{O} + \text{CO}$. The second step occurs within temperature range 306–385 °C with mass loss 10.20% (calculated mass loss = 10.13%) which could be attributed to the liberation of $\text{CH}_3\text{OH} + \text{NH}_2 + 2\text{H}_2$. DTG curve gives an endothermic peak at 358 °C. The third step is reasonably accounted for the loss of the rest of the ligand molecule $\text{C}_9\text{H}_4\text{ON}$ with estimated mass loss 27.21% (calculated mass loss = 27.66%). The total mass loss up to 486 °C is in agreement with the formation of metal acetate and few carbon atoms as the final residue (TG 49.90%, calculated 50.34%).

The TG curve of $[\text{CdHL}_1(\text{OAc})_2]\cdot 2\text{H}_2\text{O}$ with the general formula $[\text{C}_{21}\text{H}_{23}\text{N}_2\text{O}_9\text{Cd}]$ (Fig. 4), (Table 3) displays an initial mass loss in the temperature range 33–90 °C, corresponding to the decomposition of the complex to anhydrous complex by the loss of two uncoordinated water molecules. This is followed by another mass loss 70.80% (calculated mass loss = 70.66%) in the temperature range 263–480 °C corresponding to the decomposition of the ligand molecules with a final cadmium oxide residue and a total mass loss 76.90% (total calculated mass loss = 77.09%).

3.3. Electronic absorption spectra

The electronic spectra of the Schiff-base ligand HL_1 and its transition $\text{M}(\text{II})$ complexes [where $\text{M} = \text{Zn}, \text{Cd}, \text{Cu}, \text{Ni}$ and Pd] were recorded in 10^{-3} or 10^{-4} M. Within the UV spectrum of the ligand (Fig. 5), (Table 4) was observed the existence of two absorption bands assigned to the transition $\pi-\pi^*$ at 315 and 395 nm, while the longer wavelength band observed at about 450 nm can be assigned to $n-\pi^*$ transition. The copper(II) complex $[\text{CuHL}_1(\text{OAc})_2]$ exhibited one broad d–d absorption band at 685 nm, suggesting a square-planar geometry (Vančo et al., 2008). The electronic spectrum of the nickel complex $[\text{NiHL}_1\text{Cl}_2(\text{H}_2\text{O})_2]$ (Fig. 6), (Table 4) showed very

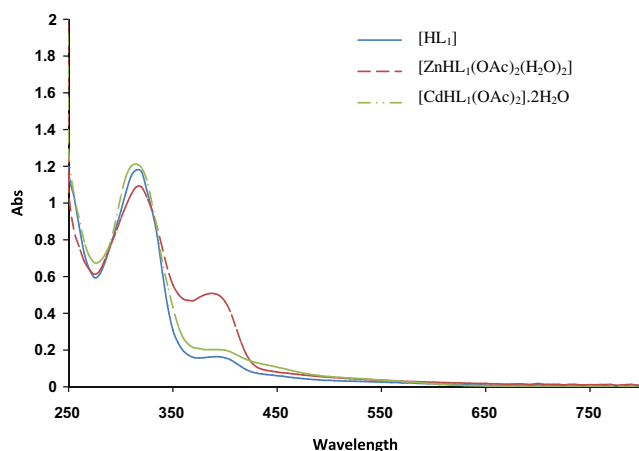


Figure 5 Electronic absorption spectra of HL_1 ligand and its $\text{Zn}(\text{II})$ and $\text{Cd}(\text{II})$ complexes in 10^{-4} M DMSO.

Table 4 Electronic absorption data of HL_1 ligand and d–d transitions of its complexes in DMSO.

Compound	Electronic transition (nm)
HL_1	315, 395, 450
$[\text{ZnHL}_1(\text{OAc})_2(\text{H}_2\text{O})_2]$	315, 395, 450
$[\text{CdHL}_1(\text{OAc})_2]\cdot 2\text{H}_2\text{O}$	315, 395, 450
$[\text{CuHL}_1(\text{OAc})_2]$	685*
$[\text{NiHL}_1\text{Cl}_2(\text{H}_2\text{O})_2]$	650(v br), 800*
$[\text{PdHL}_1\text{Cl}_2]$	465*

* d–d transition only.

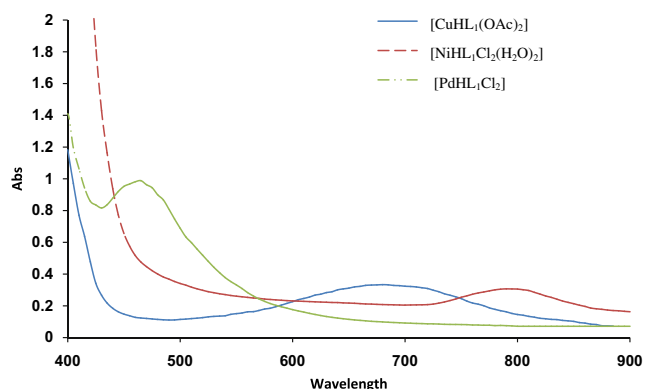


Figure 6 Electronic visible absorption spectra of $\text{Cu}(\text{II})$, $\text{Ni}(\text{II})$ and $\text{Pd}(\text{II})$ complexes of HL_1 in 10^{-3} M DMSO.

broad d–d band at 650 nm and well-defined band at 800 nm, these were assigned to the transitions $^3\text{A}_{2g}(\text{F}) \rightarrow ^3\text{T}_{1g}(\text{P})$ and $^3\text{A}_{2g}(\text{F}) \rightarrow ^3\text{T}_{1g}(\text{F})$. The lowest energy band corresponding to $^3\text{A}_{2g}(\text{F}) \rightarrow ^3\text{T}_{2g}(\text{F})$ was not observed possibly because it is outside the range of the spectrometer (at > 1000 nm). These transitions are consistent with their well-defined octahedral configuration (Vančo et al., 2008). The spectrum of $[\text{PdHL}_1\text{Cl}_2]$ complex displayed a band at 465 nm, this spin-allowed transition may correspond to $^1\text{A}_{1g} \rightarrow ^1\text{B}_{1g}$ transition indicating a square planar geometry of the metal complex. The proposed structures are summarized in Table 5 (Bon et al., 2007).

3.4. Fluorescence studies

The fluorescence spectra of the Schiff-base ligand and its $\text{M}(\text{II})$ complexes [$\text{M} = \text{Zn}, \text{Cd}, \text{Cu}, \text{Ni}$ and Pd] were studied in DMSO. The fluorescence quantum yield was determined using 7-amino-4-methylcoumarin (coumarin 120) laser dye as a reference with a known Φ_f of 0.63 in MeCN. The ligand, complexes and the reference dye were excited at 370 nm, maintaining nearly equal absorbance (~ 0.1), and the emission spectra were recorded from 350 to 600 nm (Das et al., 2007). The emission intensity was found to increase with the concentration of the ligands up to a concentration of 10^{-5} M (Fig. 7). All experiments were carried out at a concentration of 10^{-5} M. The fluorescence spectrum of the free coumarin 8-acetyl-7-hydroxycoumarin when excited at 395 nm showed a maxima band at 445 nm (blue region) with fluorescence intensity 73.473, Stokes shift $\Delta\lambda = 50$ nm and $\Phi_f = 0.47$ (Fig. 8 and

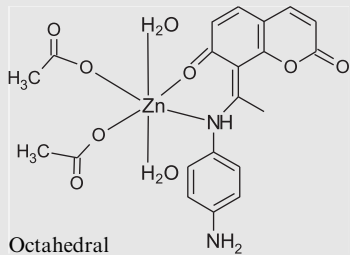
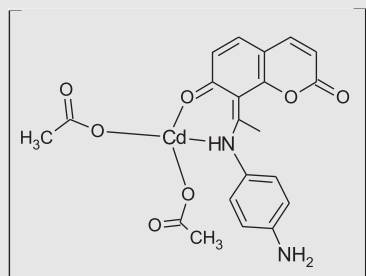
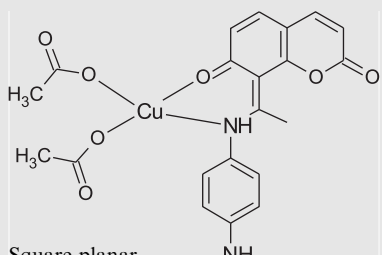
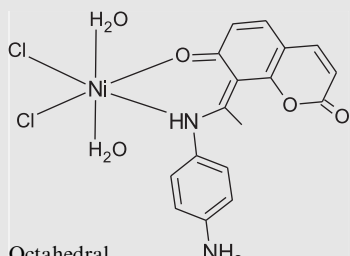
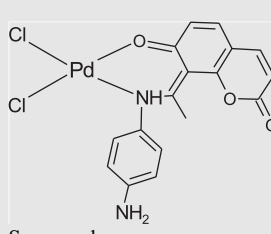
Table 5 Summary of proposed structures for metal complexes.		
Complex	Formula	Structure
[ZnHL ₁ (OAc) ₂ (H ₂ O) ₂]	C ₂₁ H ₂₄ N ₂ O ₉ Zn Pale yellow	 <p>Octahedral</p>
[CdHL ₁ (OAc) ₂].2H ₂ O	C ₂₁ H ₂₄ N ₂ O ₉ Cd Green	 <p>Tetrahedral</p>
[CuHL ₁ (OAc) ₂]	C ₂₁ H ₂₀ N ₂ O ₇ Cu Brown	 <p>Square planar</p>
[NiHL ₁ Cl ₂ (H ₂ O) ₂]	C ₁₇ H ₁₈ Cl ₂ N ₂ O ₅ Ni Green	 <p>Octahedral</p>
[PdHL ₁ Cl ₂]	C ₁₇ H ₁₄ Cl ₂ N ₂ O ₃ Pd Green	 <p>Square planar</p>

Table 6). The HL₁ ligand displayed the maximum emission bands at 446 nm (blue region) when excited at 395 nm with fluorescence intensity 193.73, Stokes shift $\Delta\lambda = 51$ nm and $\Phi_f = 0.48$. The high fluorescence quantum yield of HL₁ com-

pared to 8-acetyl-7-hydroxycoumarin may be attributed to the large dipole moment of the fluorescent excited state; other factors such as hydrogen bonds formed between HL₁ and solvent also influence the photophysical properties of the ligand.

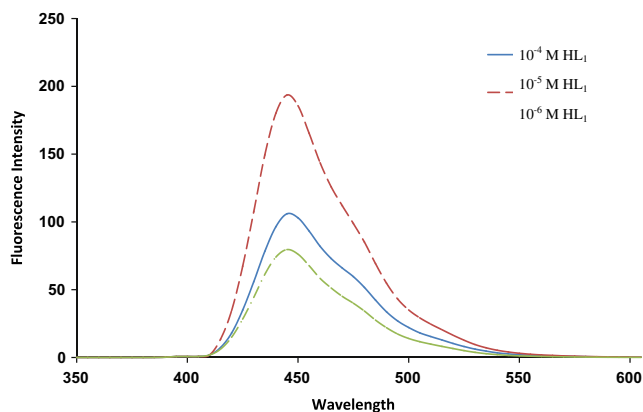


Figure 7 Fluorescence emission spectra of 10^{-4} , 10^{-5} and 10^{-6} M of HL_1 (excitation at 395 nm) in DMSO.

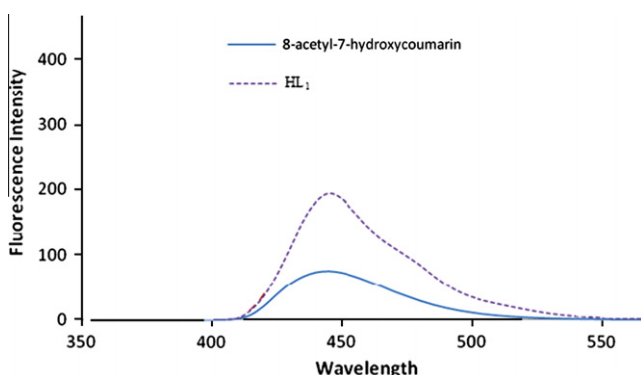


Figure 8 Fluorescence emission spectra of 10^{-5} M 8-acetyl-7-hydroxycoumarin and HL_1 (excitation at 395 nm) in DMSO.

Table 6 Fluorescence emission (λ_{em}), Stokes shift ($\Delta\lambda$) and quantum yield (Φ_f) for HL_1 ligand and its metal(II) complexes (excitation at 395 nm) in DMSO.

Compound	DMSO		
	λ_{em}	$\Delta\lambda$	Φ_f
8-Acetyl-7-hydroxycoumarin	445	50	0.47
HL_1	446	51	0.48
$[ZnHL_1(OAc)_2(H_2O)_2]$	446	51	0.50
$[CdHL_1(OAc)_2] \cdot 2H_2O$	446	51	0.49
$[CuHL_1(OAc)_2]$	443	48	0.31
$[NiHL_1Cl_2(H_2O)_2]$	445	50	0.37
$[PdHL_1Cl_2]$	445	50	0.21

The emission spectral shape of the Zn(II) and Cd(II) complexes closely resembled that of the ligand. The Zn(II) and Cd(II) complexes (Fig. 9 and Table 6) showed fluorescence emission band at 446 nm Stokes shift $\Delta\lambda = 51$ nm with fluorescence intensity 358.97 and 328.52, and $\Phi_f = 0.50$ and 0.49 for Zn(II) and Cd(II) complexes, respectively. The emission intensity of the Zn(II)-complex is stronger than that of the ligand (Yu et al., 2008). These results suggest that HL_1 may be a suitable agent to detect zinc ion. Therefore, this kind of

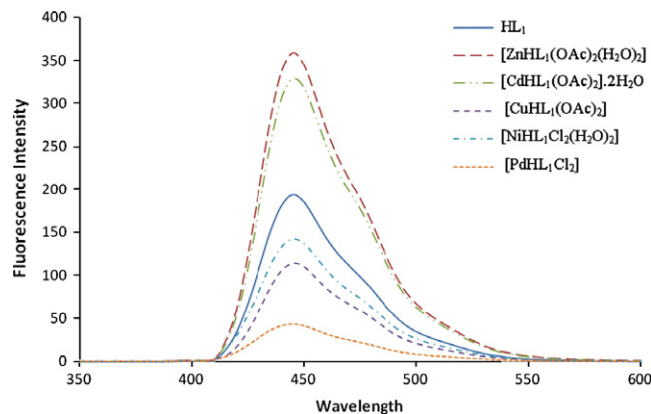


Figure 9 Fluorescence emission spectra of 10^{-5} M of HL_4 and its M(II) complexes (excitation at 395 nm) in DMSO.

compounds may have potential uses as a Zn^{2+} sensor (Wu et al., 2004). Both the Zn(II) and Cd(II) complexes exhibit strong fluorescence in comparison with HL_1 , since the Zn(II) and Cd(II) ions are difficult to oxidize or reduce due to their stable d^{10} configurations (Basak et al., 2007). On the other hand, the fluorescent intensity enhancement may be due to the coordination of free ligand to Zn(II) and Cd(II) reducing the loss of energy via radiationless thermal vibrations of the intraligand excited states and due to an increase in the rigidity of the ligand (Ye et al., 2005).

The Cu(II), Ni(II) and Pd(II) complexes (Fig. 9 and Table 6) showed fluorescence intensity 114.42, 141.97 and 43.38, and $\Phi_f = 0.31$, $\Phi_f = 0.37$ and $\Phi_f = 0.21$, respectively. The emission spectra for the complexes were characterized by the emission band around 446 nm and quenching of fluorescence intensity (Wang and Yang, 2008). Quenching of fluorescence of a ligand by transition metal ions during complexation is a rather common phenomenon which is explained by processes such as magnetic perturbation, redox activity, and electronic energy transfer (Bagihalli et al., 2008; Basak et al., 2007).

3.5. ESR studies of $[CuHL_1(OAc)_2]$ complex

The ESR spectrum of $[CuHL_1(OAc)_2]$ in DMSO at 150 K indicates that the value of $g_{||}$ (2.057) is less than g_{\perp} (2.1022) and $A_{||} = 67$ G. The spectrum exhibits features similar to the majority of other tetragonally distorted, copper complexes which is consistent with an elongation or a weaker field along the tetragonal axis. The parameter G is found to be greater than 4 (6.462) indicating that the exchange coupling between two copper centers in the solid state is negligible (EL Hussein et al., in press).

3.6. The nuclear magnetic resonance

The 1H NMR of the ligand HL_1 showed the presence of two isomers in solution in a ratio 1: 4 (Hussein et al., in press). The signal resonance at (δ 2.31 and 2.67 ppm) was assigned to azomethine methyl protons ($CH_3C=N$), thus confirming Schiff-base formation. The N-H resonance in HL_1 is broad due to the quadrupole moment of the nitrogen atom. The multiplet (doublet and triplet) resonances at 6.14–8.00 ppm were attributed to the protons of aromatic rings of both the 4-aminophenylimino and coumarin moieties. In the 1H NMR spectra

Table 7 ^1H NMR shifts for HL_1 and its Zn complex.

Compounds in $\text{DMSO}-d_6$	Chemical shifts (ppm)				
	NH_2	H_2O or NH	$\text{CH}_3\text{C}\equiv\text{N}$	Ar-H	COOCH_3
HL_1	3.31	4.42, 5.15	2.31, 2.67	6.11–7.95	–
$[\text{ZnHL}_1(\text{OAc})_2(\text{H}_2\text{O})_2]$	3.38	5.34	2.27	6.19–7.94	2.38, 2.56

of $[\text{ZnL}_1(\text{OAc})_2\text{H}_2\text{O}]$ only one isomer was observed indicating that the slow isomerization about $\text{C}\equiv\text{N}$ bond is stopped due to bonding to the metal ion (Ray and Bharadwaj, 2008). An important signal in the NMR spectrum of $[\text{ZnL}_1(\text{OAc})_2\text{H}_2\text{O}]$ is that due to the coordination of two acetyl groups occurring at δ 2.38 and 2.56 ppm thus confirming its proposed structure (Table 7).

4. Conclusion

Spectroscopic studies clearly verified the coordination ability of the ligand in complexation reaction with metal(II) ions [metal = Zn(II) , Cd(II) , Cu(II) , Ni(II) and Pd(II)]. The ligand coordinated to the metal ions through azomethine nitrogen and phenolic oxygen atoms only. The fluorescence intensity of the ligand is quenched upon complexation with metal ions such as Cu(II) , Ni(II) and Pd(II) , but enhanced more than two-fold on complexation with Zn(II) and Cd(II) in DMSO. These properties could be exploited for the detection and spectrofluorimetric determination of Zn(II) and Cd(II) in real, environmental, biological and pharmaceutical formulations. The ligand can be effectively utilized as a new sensitive chemosensor for the Zn(II) and Cd(II) ions.

Acknowledgment

The authors thank King Abdulaziz University for financial support.

References

Bagihalli, G.B., Avaji, P.G., Patil, S.A., Badami, P.S., 2008. European Journal of Medicinal Chemistry 43, 2639.

- Basak, S., Sen, S., Banerjee, S., Mitra, S., Rosair, G., Rodriguez, M.T.G., 2007. Polyhedron 26, 5104.
- Bon, V.V., Orysyk, S.I., Pekhnyo, V.I., Orysyk, V.V., Volkov, S.V., 2007. Polyhedron 26, 2935.
- Creaven, B.S., Devereux, M., Karcz, D., Kellett, A., McCann, M., Noble, A., Walsh, M., 2009. Journal of Inorganic Biochemistry 103, 1196.
- Das, D., Chand, B.G., Dinda, J., Sinha, C., 2007. Polyhedron 26, 555.
- Donia, A.M., El-Boraey, H.A., El-Samalehy, M.F., 2003. Journal of Thermal Analysis and Calorimetry 73, 987.
- Garnovskii, A.A., Nivorozhkin, A.L., Minkin, V.I., 1993. Coordination Chemistry Reviews 126, 1.
- EL Hussein, A.F., Aazam, E.S., Shehri, A.L.J.M., Al Amri, H.M., in press.
- Kachkovski, O.D., Tolmachev, O.I., Kobryn, L.O., Bila, E.E., Ganushchak, M.I., 2004. Dyes Pigments 63, 203.
- Lever, A.B.P., Ogden, D., 1967. J. Chem. Soc. (A) Inorg. Phys. Theor. 2041.
- Ray, D., Bharadwaj, P.K., 2008. Inorganic Chemistry 47, 2252.
- Refat, S.R., El-Korashy, S.A., Ahmed, A.S., 2008. Journal of Molecular Structure 881, 28.
- Vančo, J., Marek, J., Trávníček, Z., Račanská, E., Jan Muselík, J., Ol'ga Š vajlenova, O., 2008. Journal of Inorganic Biochemistry 102, 595.
- Wang, Y., Yang, Z.Y., 2008. Journal of Luminescence 128, 337.
- Wu, Z., Chen, Q., Yang, G., Xiao, C., Liu, J., Yang, S., Ma, J.S., 2004. Sensors and Actuators B 99, 511.
- Ye, Q., Chen, X.-B., Song, Y.-M., Wang, X.-S., Zhang, J., Xiong, R.G., Fun, H.K., You, X.Z., 2005. Inorganica Chimica Acta 358, 1258.
- Yu, T., Zhang, K., Zhao, Y., Yang, C., Zhang, H., Qian, L., Fan, D., Dong, W., Chen, L., Qiu, Y., 2008. Inorganica Chimica Acta 361, 233.